Remote Sensing Applications: Society and Environment 26 (2022) 100733

Contents lists available at ScienceDirect

Remote Sensing Applications: Society and Environment

journal homepage: www.elsevier.com/locate/rsase

A satellite-based Standardized Antecedent Precipitation Index (SAPI) for mapping extreme rainfall risk in Myanmar

Thong Nguyen-Huy [a,b,c,*], Jarrod Kath [b,d], Thomas Nagler [e], Ye Khaung [f], Thee Su Su Aung [f,g], Shahbaz Mushtaq [b], Torben Marcussen [b], Roger Stone [b]

[a] SQNNSW Drought Resilience Adoption & Innovation Hub, University of Southern Queensland, Toowoomba, QLD, Australia
[b] Centre for Applied Climate Sciences, University of Southern Queensland, Toowoomba, QLD, Australia
[c] Ho Chi Minh City Space Technology Application Center, Vietnam National Space Center, VAST, Ho Chi Minh, Viet Nam
[d] School of Agriculture and Environmental Science, Faculty of Health, Engineering and Sciences, University of Southern Queensland, Toowoomba, QLD, Australia
[e] Delft Institute of Applied Mathematics, Delft University of Technology, Delft, the Netherlands
[f] International Institute of Rural Reconstruction, Yangon, Myanmar
[g] Italian Agency for Development Cooperation - AICS Yangon, Myanmar

ARTICLE INFO

Keywords:
Flood monitoring
Risk management
Multivariate modelling
Vine copulas
Climate characteristics
Joint distribution
Tail dependences
Satellite-based precipitation

ABSTRACT

In recent decades, substantial efforts have been devoted in flood monitoring, prediction, and risk analysis for aiding flood event preparedness plans and mitigation measures. Introducing an initial framework of spatially probabilistic analysis of flood research, this study highlights an integrated statistical copula and satellite data-based approach to modelling the complex dependence structures between flood event characteristics, i.e., duration (D), volume (V) and peak (Q). The study uses Global daily satellite-based Climate Hazards Group InfraRed Precipitation with Station data (CHIRPS) (spatial resolution of ~5 km) during 1981–2019 to derive a Standardized Antecedence Precipitation Index (SAPI) and its characteristics through a time-dependent reduction function for Myanmar. An advanced vine copula model was applied to model joint distributions between flood characteristics for each grid cell. The southwest (Rakhine, Bago, Yangon, and Ayeyarwady) and south (Kayin, Mon, and Tanintharyi) regions are found to be at high risk, with a probability of up to 40% of flood occurrence in August and September in the south (Kayin, Mon, and Tanintharyi) and southwest regions (Rakhine, Bago, Yangon, and Ayeyarwady). The results indicate a strong correlation among flood characteristics; however, their mean and standard deviation are spatially different. The findings reveal significant differences in the spatial patterns of the joint exceedance probability of flood event characteristics in different combined scenarios. The probability that duration, volume, and peak concurrently exceed 50th-quantile (median) values are about 60–70% in the regions along the administrative borders of Chin, Sagaing, Mandalay, Shan, Nay Pyi Taw, and Keyan. In the worst case and highest risk areas, the probability that duration, volume, and peak exceed the extreme values, i.e., the 90th-quantile, about 10–15% in the southwest of Sagaing, southeast of Chin, Nay Pyi Taw, Mon and areas around these states and up to 30% in the southeast of Dekkhinathiri township (Nay Pyi Taw). The proposed approach could improve the evaluation of exceedance probabilities used for flood early warning and risk assessment and management. The proposed framework is also applicable at larger scales (e.g.,

* Corresponding author. SQNNSW Drought Resilience Adoption & Innovation Hub, University of Southern Queensland, Toowoomba, QLD, Australia.
E-mail address: thong.nguyen-huy@usq.edu.au (T. Nguyen-Huy).

https://doi.org/10.1016/j.rsase.2022.100733
Received 22 August 2021; Received in revised form 21 February 2022; Accepted 11 March 2022
Available online 6 April 2022

regions, continents and globally) and in different hydrological design events and for risk assessments (e.g., insurance).

1. Introduction

Flooding is one of the most damaging natural catastrophes. Flooding causes serious destruction to the economy, environment, and society in many areas of the world. Floods affect approximately 250 million people and cause more than USD40 billion in losses worldwide annually (OECD 2016). By 2050, average global flood losses are estimated to increase to USD52 billion per year from socio-economic changes alone and to USD60-63 billion per year when considering projected subsidence and sea-level rises (Hallegatte et al., 2013). To mitigate the significant consequences of floods, it is important to develop robust approaches and appropriate tools for accurate prediction, quantification, and risk assessment of extreme rainfall and flood events, both at gauged and ungauged locations.

Floods are extreme hydrological events, like storms and droughts, that are inevitable, complex, and stochastic in nature (Shiau 2003). Therefore, strategies based on ill-equipped models and low-quality data often result in poor flood risk management strategies. A lack of data, as well as appropriate indices or indicators integrated with multivariate models, have posed a significant challenge when modelling flood occurrence and impacts. High-quality spatio-temporal data is critical for flood modelling. Indeed, model accuracy and reliability depend on the availability and accuracy of the data. Studies analysing flood characteristics using daily streamflow discharge records often rely solely on data from gauging stations. However, difficulties arise from the fact that many regions in the world, particularly in developing countries, have no data or only a sparsely scattered station network to collect the data. In practice, extreme events such as floods and droughts may occur in different locations at the same time, and as such can represent a systemic risk (Nguyen-Huy et al., 2019). If analyses are restricted only to areas with station data, the spatially complex and systemic nature of flood risks may be overlooked. As such, areas lacking long-time series of station data need approaches for quantifying flood characteristics.

To overcome the issues of absent station data on flood risks, free satellite data sources, such as Moderate Resolution Imaging Spectroradiometer (MODIS), Landsat, and Sentinel, have been widely applied for flood mapping and monitoring to inform disaster risk management (Ganaie et al., 2013; Memon et al., 2015). In general, these satellite indices are derived from optical spectral bands (MODIS and Landsat) such as Normalized Different Water Index (NDWI) (McFeeters 1996), Water Index (WI) (Rogers and Kearney 2004; Ji et al., 2009), Land Surface Water Index (LSWI) (Xiao et al., 2004), and from radar backscatter values such as Normalized Difference Flood Index (NDFI) (Cian et al., 2018). The applications of these indices provide wide and long-term spatio-temporal coverage of flood patterns suitable for identifying hotspots and risk assessment.

Regarding flood indices or indicators, it is well known that flood risk assessment should be based on how the remaining quantity of water due to heavy precipitation fluctuates over time and whether flood indicators can reciprocate changing hydrological conditions. It is also noted that the start and end dates of flood events and monitoring can be spontaneous, short-term, or chronic, and hence flood monitoring should be based on antecedent precipitation in each period. This is not achievable using precipitation data alone or other indices such as the Standardised Precipitation Index (SPI) (McKee et al., 1993; Seiler et al., 2002) that focus on precipitation distribution on monthly or annual scales. For example, if a flash flood event had occurred, such indices are not available until the last day of the monthly period when statistical analyses of cumulative precipitation are completed. Another issue with using precipitation data alone or equal-weighted indices (e.g., SPI) is that the precipitation recorded in days before that period is not considered objectively and so this may lead to an inaccurate estimate of the changes in water reserves that are vital in elevating or reducing the flood risk. Instead, an index based on the unevenly weighted contribution of a series of heavy precipitation events is potentially more useful and a better assessment of risk.

Floods are complex events and hence univariate frequency analysis can only provide limited information of these events and may lead to an overestimation or underestimation of flood-related risks (Yue et al., 2001; Shiau et al., 2006). Consequently, describing flood events through multiple characteristics such as volume (V), flood peak (Q), and duration (D) is needed for a better understanding of these complex and interacting flood processes. For example, if a flood risk assessment is based only on duration, then high peak and volume risks will be missed. Instead, it is the combined, or co-occurrence, of extreme volume, peak and duration flood events that are likely to cause the most damage and therefore should be a priority for risk assessments. Further, as flood characteristics are generally interdependent, they should be jointly considered in multivariate analysis to provide a complete assessment of the true probabilities of occurrence (Chebana and Ouarda 2009).

Based on the analysis of research gaps and challenges, this study aims to develop a framework of multivariate flood frequency analysis that takes into account the advantages of advanced high-resolution remotely sensed data and statistical copula-based techniques. The proposed approach is applied for probabilistic analysis of flood characteristics for Myanmar, a southeast Asian county that has frequently suffered from severe floods (Khaing et al., 2019). Thus, the main motivation of the present study is not to develop a comprehensive flood model that often requires more input data such as land use and land cover, elevation, slope, river network, and drainage system. Instead, we outline a generalizable approach using a satellite-based antecedence precipitation index as a flood indicator and models the joint exceedance probability of flood characteristics based on this.

A flood indicator and its multiple characteristics (V, Q, D) are computed from satellite-derived precipitation using a time-dependent reduction function. Vine copulas (see methods for details) are then applied for modelling the joint distributions between extreme flood characteristics to derive important information for flood risk management including the exceedance probability, conditional probability, and return period. More details are described in the remainder of this paper organised as follows. Section 2 provides the satellite-based data sources, data pre-processing and explained the methodologies for deriving flood index and its characteristics and copula

models, and the equations for computing probabilities and return periods. Section 3 represents the main results. Section 4 discusses implications, limitations, and areas for future research. Section 5 summaries the findings and contributions of this study.

2. Materials and methods

2.1. Dataset

Daily gridded precipitation dataset was acquired from the gauge-corrected Climate Hazards Group InfraRed Precipitation with Station data (CHIRPS, version 2.0) during the period of 1981–2019 (Funk et al., 2015). The CHIRPS dataset is a 35+ year quasi-global rainfall data set covering 50°S-50°N (and all longitudes) and ranging from 1981 to near-present. CHIRPS incorporates in-house climatology, CHPclim, 0.05° resolution satellite imagery, and in-situ station data to create gridded rainfall time series (mm/day).

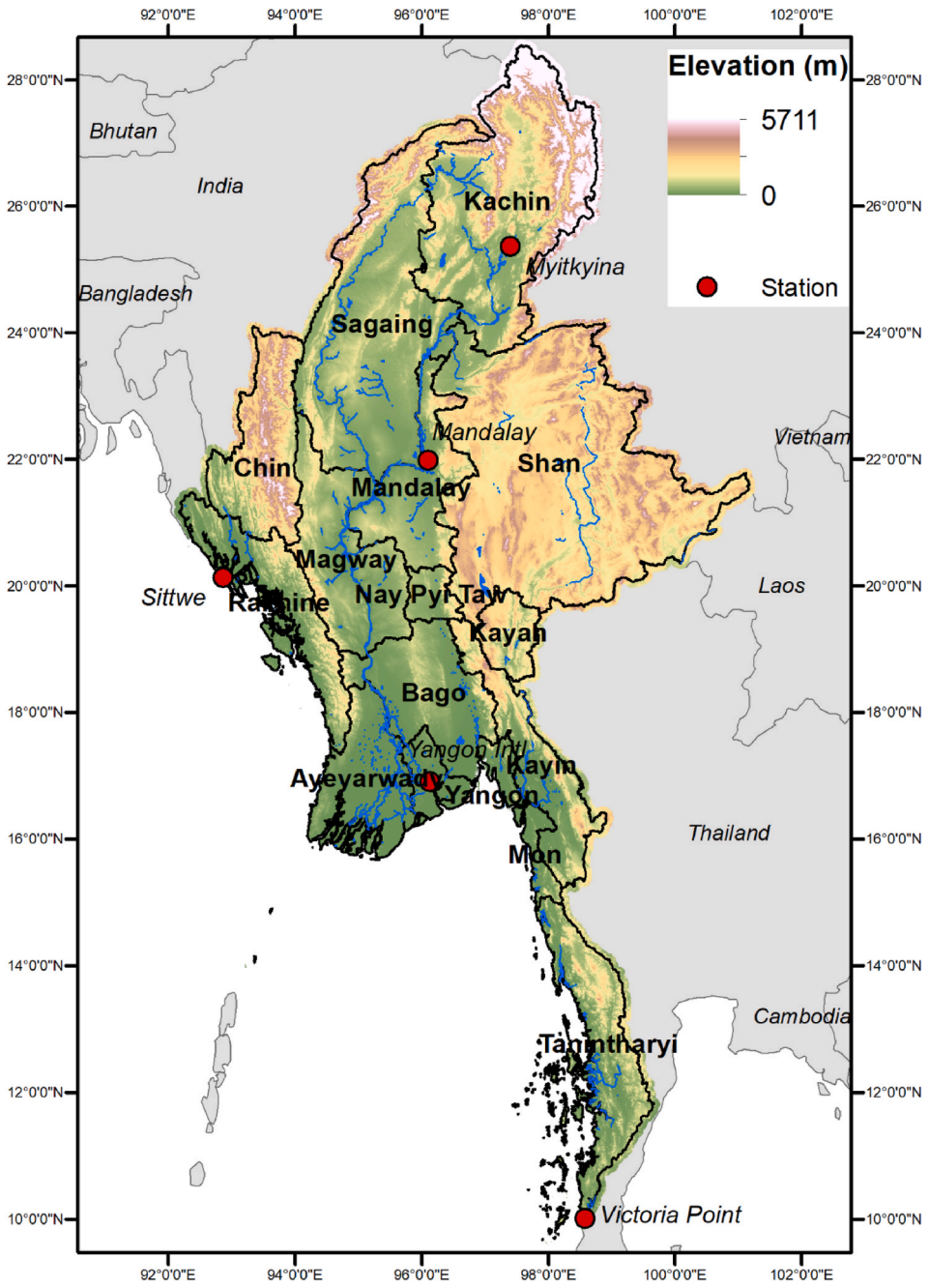

Fig. 1. Myanmar river network (blue lines) overlaid on the digital elevation model (in meter above sea level) acquired from Environment Operations Center (www.gms-eoc.org) based on Version 4.1 of NASA's Shuttle Radar Topographic Mission (SRTM) elevation dataset. Location of five stations used for validation.

The CHIRPS dataset has been evaluated and validated on a semi-global domain (126°W-153°E) (Funk et al., 2015) and global scale (Shen et al., 2020) using the gauge-based GPCC (Global Precipitation Climatology Center) data. Their results reported that the CHIRPS has a low bias and agrees well with the gauge-based GPCC. More specifically, global assessment results show that CHIRPS has negative biases of 2.01% before 2000, however, this systematic underestimation was effectively eliminated after 2000 (Shen et al., 2020). In addition, when compared to other four widely-used precipitation models and observational products, such as the Coupled Forecast System (CFS), CPC Unified interpolated gauge products (CPCU), European Center for Medium-Range Weather Forecast (ECMWF), and TRMM-based TMPA 3B42 RT, CHIRPS has lower systematic biases (Funk et al., 2015).

The evaluation and validation of CHIRPS have been also performed in many regions and countries, for example, over eastern Africa (Dinku et al., 2018), China (Bai et al., 2018), India (Gupta et al., 2020), Argentina (Rivera et al., 2018), Brazil (Paredes-Trejo et al., 2017), and Vietnam (Le et al., 2020). In general, the CHIRPS performance was found to be comparable to that of the gauge-based observations and can support effective hydrologic applications. Luo et al. (2019) reported that CHIRPS yields good performance on precipitation estimation in the Lower Lancang-Mekong River Basin. The author also concluded that CHIRPS data was superior to rain gauge and interpolated data for driving the hydrological model, particularly for large data-poor or ungauged watersheds, and river basins where observed precipitation are difficult to collect. The CHIRPS dataset has been also applied in many hydrological topics, such as drought monitoring (Gao et al., 2018; Perdigón-Morales et al., 2018), evaluation of extreme rainfall (Cavalcante et al., 2020; Gupta et al., 2020).

The validation and applications of the CHIRPS dataset have also been performed in Myanmar. Kyaw et al. (2020) indicated that CHIRPS rainfall estimates consistently agree well with ground-based rainfall at different spatiotemporal scales and are even more accurate than single stations at a large catchment scale. Acierto, Kawasaki and Zin (2020) evaluated the CHIRPS data against the 25 rain gauge stations in Myanmar. The evaluation results shown a good correlation ranging from 0.78 to 0.94. The findings also indicated that when compared to both the rain gauge monthly climatology and daily distribution data, the CHIRPS dataset shown better rainfall estimates than APHRODITE data (Asian Precipitation - Highly-Resolved Observational Data Integration Towards Evaluation) that is interpolated from in-situ measurements. The author summarized that CHIRPS is a good alternative for a gridded proxy observation over the Myanmar region. Dutta (2018) used CHIRPS data to study the impact of insufficient precipitation conditions on vegetation stress conditions in the Dry Zone of Myanmar. The author found a strong statistical correlation ($R^2 = 0.74$ and 0.82) between precipitation derived from CHIRPS data and MODIS Normalized Difference Vegetation Index (NDVI). Recently, MacLeod et al. (2021) has used CHIRPS data to evaluate the skill of ensemble forecast of extreme rainfall events over Myanmar.

The global CHIRPS dataset was then extracted for the study area, i.e., Myanmar, using its country boundary. Fig. 1 shows the river network overlaid on the digital elevation model of Myanmar acquired from Environment Operations Center (www.gms-eoc.org) based on Version 4.1 of NASA's Shuttle Radar Topographic Mission (SRTM) elevation dataset.

2.2. Standardized available precipitation index

The Standardized Antecedent Precipitation Index (SAPI) is a standardized index for meteorological flood analysis (Nguyen-Huy et al., 2020; Prasad et al., 2020) and can be used to compute flood characteristics, i.e., peak (Q), volume (V), and duration (D) on hourly, daily, and monthly timescales (Deo et al. 2015, 2018). The SAPI was originally introduced by (Byun and Lee 2002) to overcome the drawbacks of other indices, for example, derived by fitting to parametric probability distribution functions.

The computation of SAPI is based on the concept of effective (or accumulated) precipitation P_E that is the summed value of precipitation for the current day and antecedent day determined by a time-dependent reduction function (Byun and Lee 2002) through Eqs. (1)–(3):

$$P_E = \sum_{n=1}^{i} \left(\frac{\sum_{m=1}^{n} P_m}{n} \right), \tag{1}$$

$$API = \frac{P_E}{\sum_{n=1}^{i} (1/n)}, \tag{2}$$

$$SAPI = \frac{API - MEAN(\max API)}{STD(\max API)}, \tag{3}$$

where P_m is the precipitation of m days before, i represents the duration of the summation of the antecedent period, and API means an extensive measure to indicate the amount of current and accumulated precipitation in which daily reduction (by runoff, evapotranspiration, infiltration, etc.) of water, and the duration of accumulation into account quantitatively. maxAPI denotes the annual maximum value of API where *MEAN* and *STD* are the mean and standard deviation of API, respectively, for the study period. When SAPI >0 then there is an elevated risk of flooding.

In this study, the SAPI was computed for every pixel (at a 0.05° resolution) for all of Myanmar using the CHIRPS dataset between 1981 and 2019. The duration of the summation is 365 days as for the usual hydrological cycle (366 days for the leap years) and so, if we denote $W \equiv 1 + \frac{1}{2} + \frac{1}{3} \ldots + \frac{1}{365}$ as a weighting factor summed over an annual precipitation cycle, Eqs. (1) and (2) can be written as (Deo et al., 2018):

$$API = P_1 + \frac{[P_2(W-1)]}{W} + \frac{[P_3(W-1-\frac{1}{2})]}{W} + \ldots + \frac{[P_{365}(W-1-\frac{1}{2}-\ldots-\frac{1}{364})]}{W} \approx P_1 + 0.85P_2 + 0.77P_3 + \ldots + 4.23\times10^{-4}P_{365}. \quad (4)$$

According to Eq. (4), the antecedent precipitation is represented in a rational form associated with reduced weights to take into account the loss of available water resources over time. That means the index accounts for 100% of precipitation received a day before, ≈ 85% of that received two days before, ≈ 77% of that received three days before, and so on, to ≈0.0423% of that received 365 days before (Fig. 2 (a)). The model puts the highest weight on present precipitation whereas previous days' contributions decrease gradually, e.g., over an annual cycle (N = 365 days) as in this study. It is also noted that the hydrological cycle can be adjusted to specific target days depending on the objective, e.g., 10 days.

2.3. Flood characteristics

The definitions of flood characteristics, concordant with run theory (Yevjevich 1967), are illustrated in Fig. 2 (b). More specifically, the duration (D) (day) is defined as consecutive days of SAPI above zero where the first and last dates are called the onset and end date, respectively. Within a duration, the volume (V) is the cumulative SAPI, and the peak (Q) is the maximum value of SAPI.

Fig. 2 (b) also shows an example of the SAPI time series for Bilin town (17.225° N, 97.225° E) in Mon state, Myanmar from July 01, 2019 to October 31, 2019. It is worth pointing out that the onset date, i.e., when SAPI starts being above zero, was on August 06, 2019.

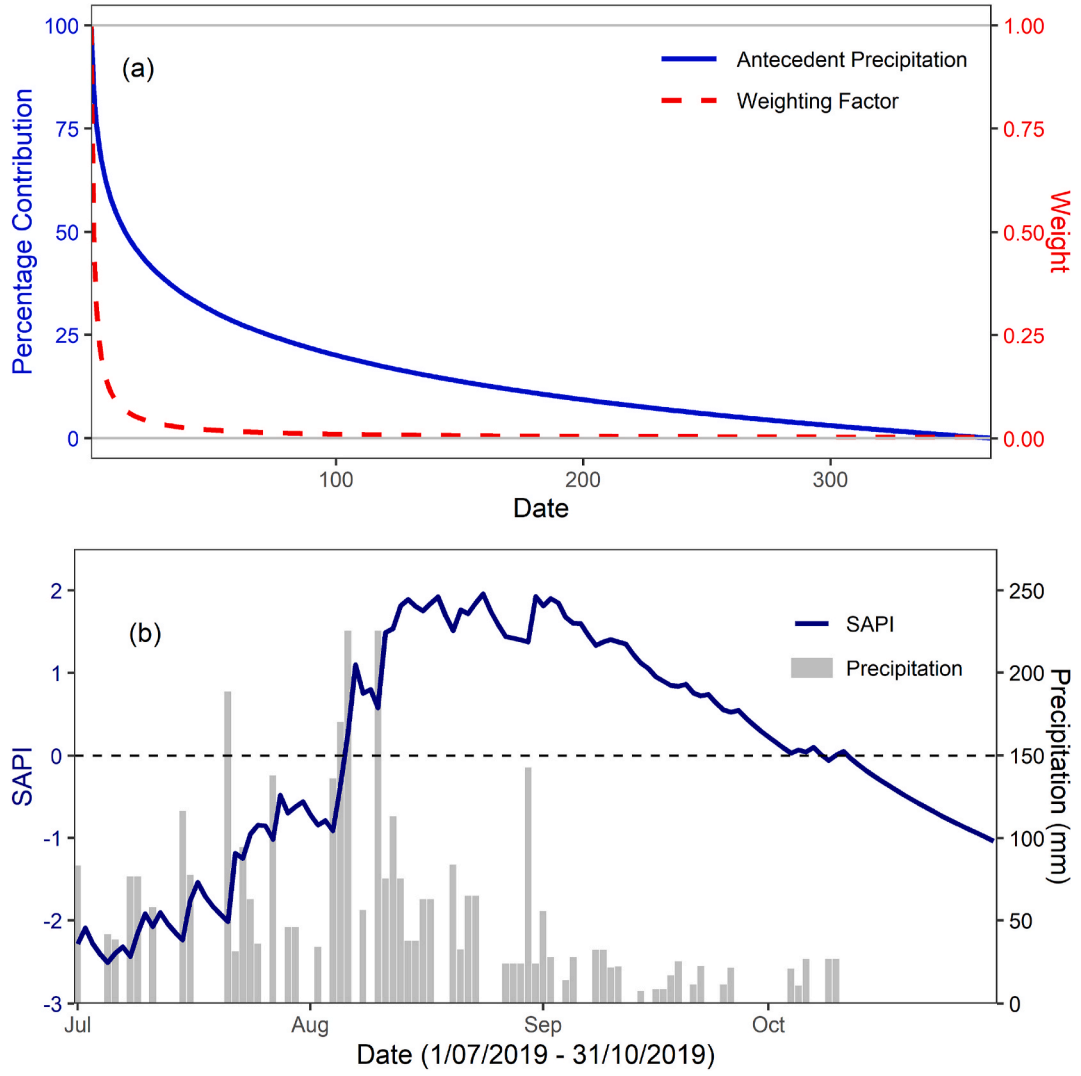

Fig. 2. (a) The time-dependent reduction function showing ratio of weighted contribution of raw precipitation (P) into effective precipitation (P_E) over annual cycle (N = 365 days). (b) An example of duration, volume, and peak of the Standardized Antecedent Precipitation Index (SAPI) time series extracted at Bilin town (17.225° N, 97.225° E) in Mon state, Myanmar. A flood event is defined as when SAPI >0.

According to the Department of Meteorology and Hydrology of Myanmar, the observed water level condition of Bilin river at Bilin reached the danger level on August 07, 2019 (FloodList 2019). Thus, using the criterion of SAPI >0 provides a good indicator of flood risk in this instance.

2.4. Exceedance probability

In hydrology, different risk analyses and assessments are performed to obtain desired information about flood behaviour. For example, conventional risk analysis of flood characteristics is generally based on one variable of interest (duration, volume, or peak) by fitting a parametric univariate distribution to that variable. In bivariate cases, one may be interested in the probability of exceeding both duration and volume. To acquire a comprehensive risk assessment, the present study analyses a multivariate case of flood characteristics, i.e., the exceedance probability of duration-volume-peak for the entire Myanmar. More specifically, we estimate the probability that duration, volume, and peak are simultaneously greater than or equal to some threshold scenarios, i.e.:

$$P(D \geq d, V \geq v, Q \geq q) = 1 - P(D < d, V < v, Q < q). \tag{5}$$

Eq. (5) requires modelling a joint distribution of such three variables, $F(x_d,x_v,x_q)$. The multivariate normal distribution is a common method used, however, not appropriate as mentioned earlier. Thus, we develop a copula-based model, which is described in the following sections, to estimate the exceedance probability of flood events.

2.5. Copulas

2.5.1. Copulas and multivariate flood analyses

The application of multivariate analysis to study flood problems has been often restricted in practice because of the limited number of techniques available for multivariate extreme modelling (Shiau et al., 2006). Furthermore, multivariate modelling, compared to univariate modelling, often requires much more data and sophisticated mathematical analysis. As a result, bivariate distributions, including but not limited to normal, logistic, exponential, gamma, and Gumbel mixed model, are commonly applied for modelling the correlation between flood characteristics (Shiau 2003; Karmakar and Simonovic 2008; Chebana and Ouarda 2011; Dong et al., 2019). However, these types of bivariate distributions exhibit some limitations. For example, the Gumbel mixed model restricts the correlation of random variables in a certain range, between 0 and 2/3 (Shiau 2006). Other drawbacks in using these bivariate distributions are that (i) each marginal distribution must come from the same family, (ii) extensions to multivariate cases are not clear, and (iii) the same parameters are used for modelling the marginal distributions and the dependence between the random variables (Favre et al., 2004). Also, the use of a multivariate normal distribution is not appropriate to model extreme variables in most cases since the marginal distributions are asymmetric, and their dependence structure is often different from the Gaussian case described by Pearson's correlation coefficient.

Copulas, introduced by Sklar (1959), offer efficient algorithms for modelling multivariate distributions that overcome the drawbacks mentioned above. More specifically, copulas are able to model the dependence structure between random variables separately with the marginal distributions. This means that each variable can come from any distribution type and their dependence structure can be either linear or non-linear. Consequently, copula-based methods have been broadly used in different fields to construct multidimensional distributions, for example in finance and insurance (de Melo Mendes, Semeraro & Leal 2010; Jaworski et al., 2013), weather forecast (Ali et al., 2018; Nguyen-Huy et al., 2020), and agriculture and climate risk (Nguyen-Huy et al., 2018; Nguyen-Huy et al., 2020). In the hydrological domain, bivariate and trivariate copulas are common approaches for jointly modelling the characteristics of extreme events such as droughts (Mirabbasi et al., 2012; Yusof et al., 2013; Saghafian and Mehdikhani 2014; Vergni et al., 2015) and floods (Zhang and Singh 2006; Karmakar and Simonovic 2009; Reddy and Ganguli 2012; Latif and Mustafa 2020a). Among multivariate copula models, vine copulas offer the most flexible way for modelling the dependence structure through bivariate building blocks (Aas et al., 2009). Recently, vine copulas have been demonstrated to outperform other traditional Archimedean and elliptical copulas in modelling flood event characteristics (Daneshkhah et al., 2016; Shafaei et al., 2017; Tosunoglu et al., 2020).

2.5.2. Copula analytical approach

A copula $C(.) : [0,1]^n \rightarrow [0,1]$ is a function that links univariate marginal distribution functions $P(X_i \leq x_i) = F_i(x_i)$ of random variables $X_1, ..., X_n$ to form a joint cumulative distribution function (JCDF) $P(X_1 \leq x_1, ..., X_n \leq x_n) = F(x_1, ..., x_n)$, i.e.:

$$F(x_1, ..., x_n) = C[F_1(x_1), ..., F_n(x_n)], \tag{6}$$

with the corresponding joint density distribution function (JPDF):

$$f(x_1, ..., x_n) = \left[\prod_{i=1}^{n} f_i(x_i)\right] c[F_i(x_i), ..., F_n(x_n)]. \tag{7}$$

here, $f_i(x_i)$ and $c(.)$ are the corresponding marginal and copula PDFs, respectively. If the marginal distributions are continuous, then the copula is unique. Eqs. (5) and (6) indicate an advanced feature of using copulas that a JCDF of random variables can be constructed by two separate processes: (i) modelling a copula function that captures the dependence structure between correlated variables, and (ii) modelling univariate marginal distributions. This advantage of copulas offers a more flexible way to select appropriate univariate distribution functions to fit the observed data in practice.

From Eq. (6), the joint distribution of duration, volume and peak mentioned in Eq. (5) can be expressed in terms of copulas as:

$$P(D \geq d, V \geq v, Q \geq q) = 1 - F(x_d, x_v, xq) = 1 - C\left[F_D(x_d), F_V(x_v), F_Q\left(x_q\right)\right]. \quad (8)$$

The copula function in Eq. (8) may be modelled by different copula families including, but not limited to, empirical, Archimedean, extreme value, elliptical, vine, and entropy copulas. Vine copulas, introduced in more details in the following section, among others, offer the most flexibility to construct the JCDF and JPDF as shown in Eqs. (6) and (7), respectively.

2.6. Vine copulas

Introduced by Joe (1996) and developed further by Bedford and Cooke (2002), the vine approach decomposes the JPDF into a cascade of iteratively conditioned bivariate copulas, so-called the pair copulas (Aas et al., 2009). The vine copula can be expressed in three forms: drawable-vine (D-vine), canonical-vine (C-vine), and regular-vine (R-vine).

To be consistent with the scope of the study for modelling the joint distribution of flood duration, volume, and peak, we take the trivariate case as an example for illustration. Fig. 3 graphically described examples of the D- and C-vine copulas in a form of trees, edges, and nodes. In the trivariate case, the C-vine copula is the D-vine copula with a given center variable, for example, with the duration (D) variable as the center, the D-vine copula in Fig. 2(b) is exactly the same as the C-vine copula in Fig. 2(d). The edges are identified with bivariate copulas, for example, the edge *DV* associated with the bivariate copula C_{DV} that models the dependence structure between *D* and *V*. The JPDF in Eq. (6) can be written as (Czado 2019):

$$f(v, d, q) = f_V(v) f_{D|V}(d|v) f_{Q|V,D}(q|v, d), \quad (9)$$

where:

$$f_{V|D}(d|v) = c_{DV}[F_D(d), F_V(v)] f_V(v), \quad (10)$$

$$f_{Q|V,D}(q|v, d) = c_{VQ|D}\left[F_{V|D}(v|d), F_{Q|D}(q|d)\right] f_{Q|D}(q|d), \quad (11)$$

$$F_{Q|D}(q|d) = \frac{\partial C_{DQ}[F_D(d), F_Q(q)]}{\partial F_D(d)} \quad (12)$$

$$F_{V|D}(v|d) = \frac{\partial C_{DV}[F_D(d), F_V(v)]}{\partial F_D(d)}. \quad (13)$$

For fitting the univariate marginal distribution functions, we applied the univariate local-polynomial likelihood kernel density estimation (Nagler, T & Vatter, T 2018) that can handle both discrete (duration) and continuous (volume and peak) data (Nagler, 2018a, 2018b). Also, all bivariate copula families are employed for modeling the vine copulas including independence, parametric (elliptical, Archimedean and their rotated versions), and non-parametric (transformation kernel) families (Nagler and Czado 2016; Nagler et al., 2017). For the estimates of bivariate copula parameters, the maximum likelihood and local-likelihood approximations were applied for parametric and non-parametric models, respectively. Additionally, the Akaike information criterion (AIC) and Kendall's tau were adopted as the criterion for selecting the bivariate copulas and tree sequences. For more details, readers are referred

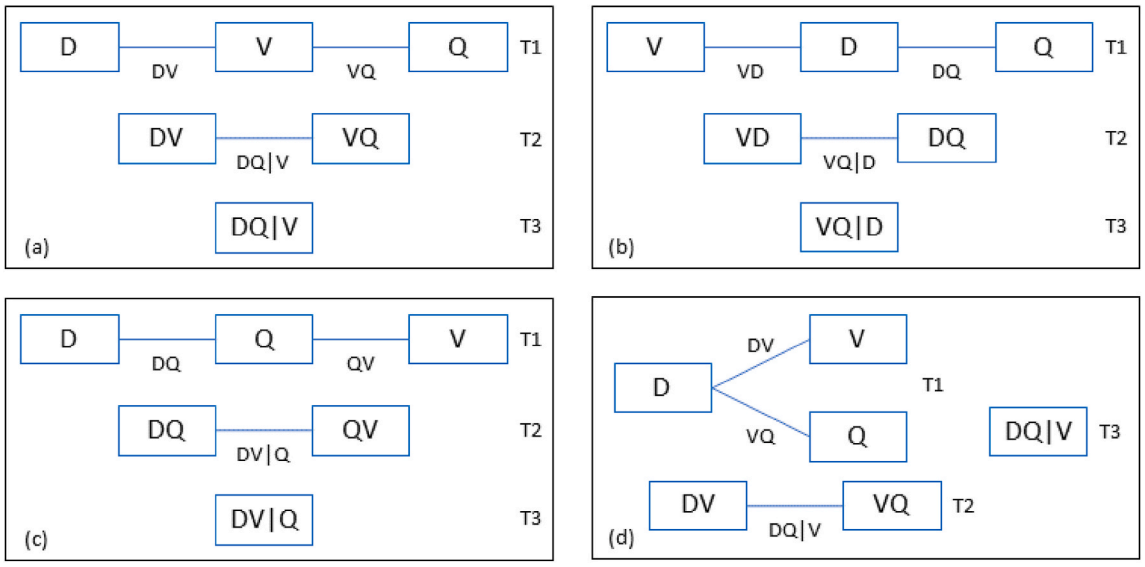

Fig. 3. Example of 3-dimensional D-vine (a–c) and C-vine (d) copula with 3 trees and 3 edges where duration (D), volume (V), and peak (Q) are nodes. Each edge is associated with a pair-copula.

to the work by Nagler, Thomas and Vatter, Thibault (2018). All the computations of this paper were implemented using the R programming language.

3. Results

3.1. Exceedance probability of SAPI characteristics

The Standardized Antecedent Precipitation Index (SAPI) and its characteristics were calculated for each gridded cell separately over all of Myanmar. Annual maximum values of SAPI are presented in Fig. S1 in supplementary. It can be seen that SAPI is able to capture heavy rainfall events, potentially leading to flood events that occurred in the past, e.g., the occurrence of significantly wet conditions in 1994, 2001, 2002, 2006, 2010 and 2011. Fig. 4 shows the number of times that SAPI >0, which is an indicator of flood events, over the period of 38 years (1982–2019). In general, except for some regions in the center, flood potentially occurs at least once a year in a major part of Myanmar. It is noticed that the extreme event numbers in the southwest states including Bago, Ayeyarwardy, and Yangon and Kachin state in the north are extremely high, up to 3 times per year on average. Some regions in other states such as Shan, Sagaing, and Rakhin also expose a high risk of occurring heavy rainfall events.

Fig. 5 represents the probability that SAPI is above zero in the rainy monsoon season (Jun–Oct), which is $P(FI > 0) = 1 - P(FI \leq 0)$, where $P(FI \leq 0)$ derived from the empirical cumulative distribution function. The results are in agreement with annual observations in Myanmar, reported by ADPC (2009), where during the rainy season flooding regularly occurs in three waves: June, August, and late September to October with major hazards arriving in August as peak monsoon rains occur around that time. The result indicates the highest probability (up to 40%) of flood occurrence in August and September in the south (Kayin, Mon, and Tanintharyi) and southwest regions (Rakhine, Bago, Yangon, and Ayeyarwady). The high chance of flood occurrence (up to 25%) is also found for the northern parts of Sagaing and Kachin in Sep and in the central part (south of Sagaing) in October. These maps of a high chance of flood occurrence coincide well with the maps of flood-prone areas in Myanmar shown in Fig 18 in the report of UoM (2009) (see Section 6.3, page 50).

The statistics of SAPI duration, volume, and peak including mean, standard deviation, skewness, and kurtosis are illustrated in Figs. S2 and S3 (supplementary). In general, the majority of Myanmar has an average duration of about 4–10 days of rainfall surplus, i.e., consecutive days of SAPI above zero. However, this is even high, between 16 and 24 days, in the south and southwest regions (Fig. S2). Accordingly, those regions also have the highest average volume. However, while the central and southeast regions have lower values of duration, these regions also have high values of average volume. The standard deviation of duration and volume reveals a similar pattern, i.e., higher values in the lower part (south, southeast, and southwest). The highest average peak and its standard deviation can be observed in the center spanning from the west to east. The high spatio-temporal variability of the duration, volume and peak of extreme events highlights the importance of modelling these characteristics simultaneously.

Fig. S2 also presents the skewness and kurtosis information of duration, volume, and peak, which is useful information for

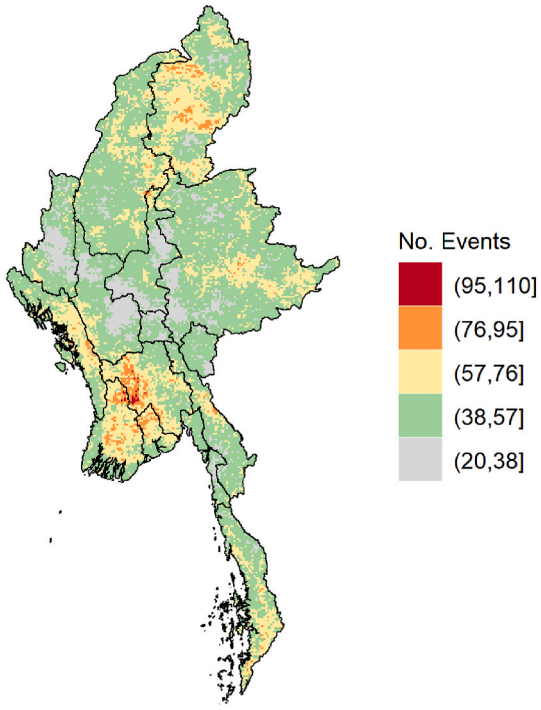

Fig. 4. Number of times that the Standardized Antecedent Precipitation Index (SAPI) is above 0, which is an indicator of flood events, over a period of 38 years (1982–2019).

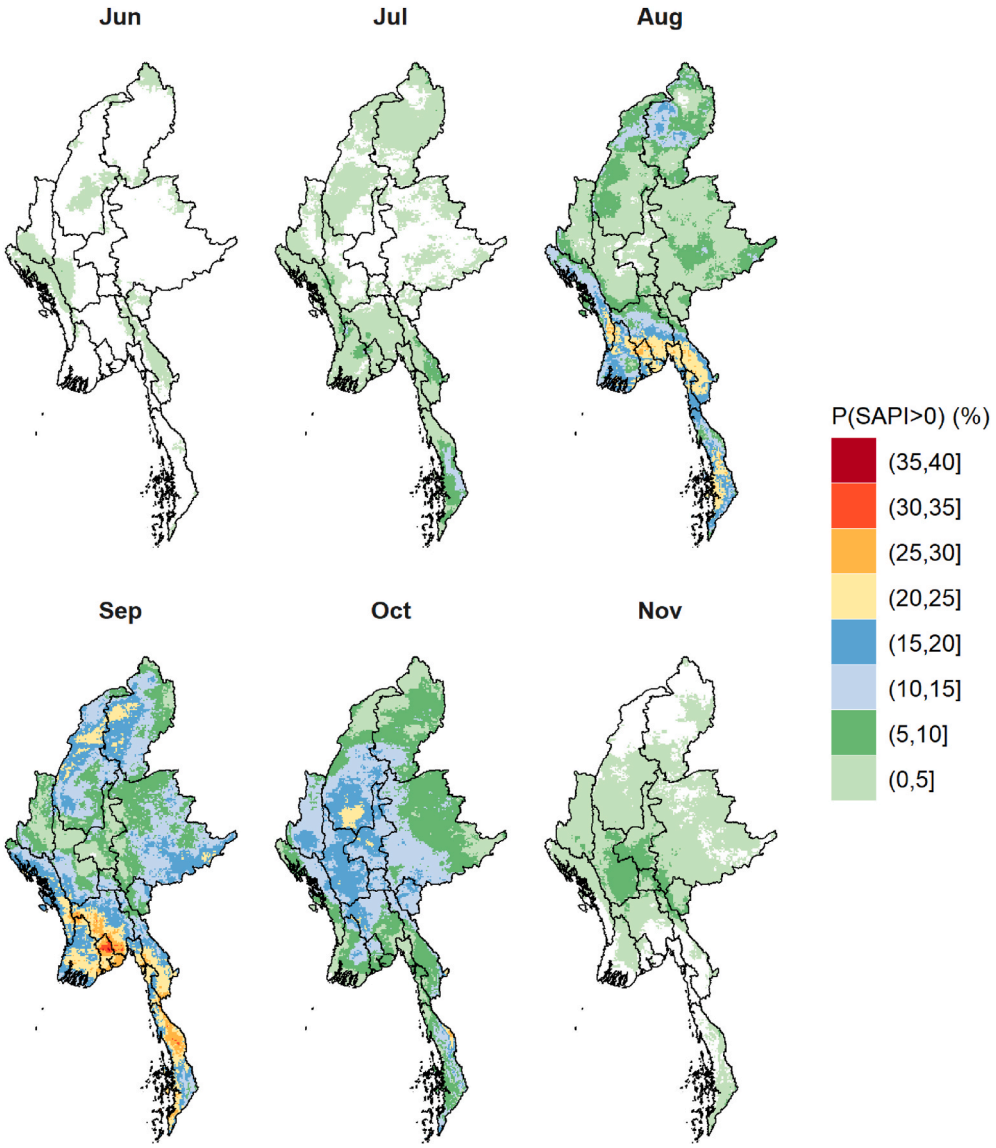

Fig. 5. The probability that the Standardized Antecedent Precipitation Index (SAPI) is above zero, which is an indicator of a flood event, in Myanmar in the rainy monsoon season (Jun–Oct) over 38years (1982–2019).

understanding the pattern of the data, i.e., the probability distribution of each characteristic. Skewness is a measure of whether the distribution is symmetric or asymmetric relative to its means. Kurtosis is a measure of whether the data are heavy-tailed or light-tailed relative to a normal distribution. From Fig. S2, the skewness and kurtosis of the majority data are much greater than +1 and + 3 indicating that the distributions of flood characteristics are highly skewed right. Such right-skewed distributions reflect a large range of extreme values of flood duration, volume, and peak. These findings also emphasize the need for a robust model, such as copulas used in this study, to fully capture the dependence between those characteristics.

Analysing the correlation among duration, volume and peak is another important step in modelling the joint distribution among these variables. Different correlation coefficients between the characteristic pair are computed to have a complete analysis of their relationship. The Pearson correlation coefficient measures the strength of a linear association between two variables where its nonparametric version, the Spearman's rank correlation coefficient, and Kendall's tau measure the strength and direction of association between the rank values of those two variables. It is also noted that the values of Kendall's tau are usually lower than those of the Spearman's rank.

The results shown in Fig. 6 indicate a strong positive relationship among the flood characteristics in all measures where the values of correlation coefficients range between a Pearson r of 0.4–1. The p-values of the significance level of the *t*-test are also computed (not shown here) are less than the significance level alpha of 0.05 indicating that the three characteristics are significantly correlated together. The correlation between duration and volume is found to be spatially consistent in all measures where the values of Kendall's

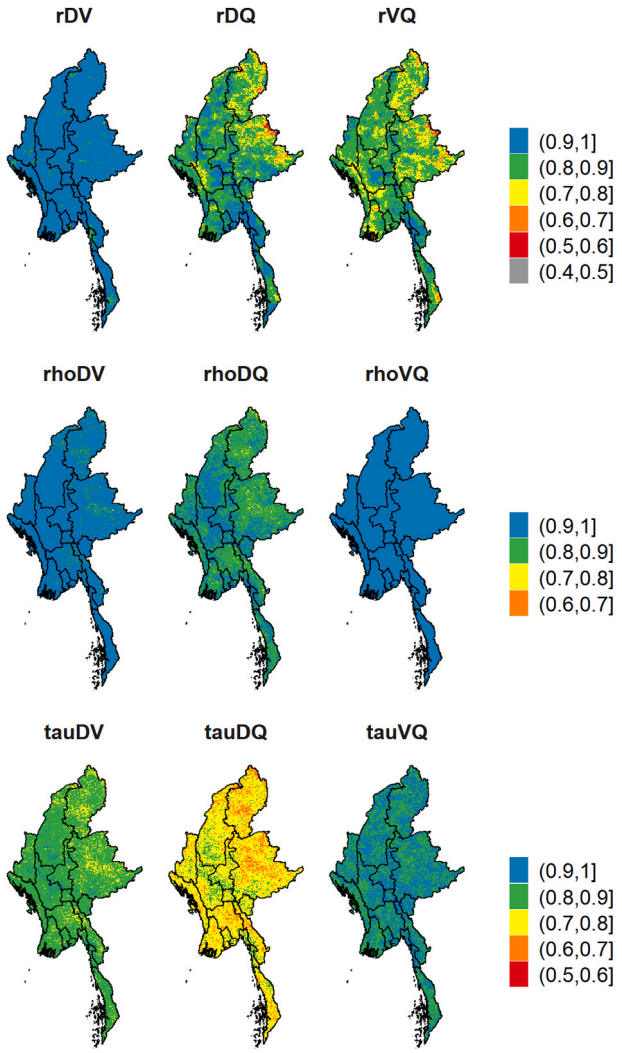

Fig. 6. Spatial patterns of Pearson (top), Spearman's rank (middle), and Kendall's tau (bottom) correlation coefficients between pairs of Standardized Antecedent Precipitation Index (SAPI): duration (D), volume (V), and peak (Q).

tau are slightly lower than those of the Spearman's rank, which is expected. The correlation coefficients between duration-peak and volume-peak are more spatially variable where their values in the north and northeast regions are considerably lower than those figures in the rest parts. In addition, the Pearson's correlation coefficients between duration-peak and volume-peak are lower than those measured from the rank methods. These findings imply a strong monotonic relationship between flood peak with duration and volume. In other words, when the duration or volume increases, the peak increases at a non-constant rate that differs from the linear relationship.

Copula functions are able to fully capture the complicated dependence between variables regardless of their relationship patterns. By modelling the joint distribution between flood characteristics using vine copulas, the joint exceedance probability was derived for different combination scenarios of extreme events using Eqs. (8) - (13). More specifically, we quantify the probability that duration, volume, and peak exceed specific thresholds concurrently. The thresholds were selected at 50th-quantile (median), 75th-(moderate), and 90th-quantile (extreme) averaged for the entire country. As can be seen in Table 1, for example, the averaged 50th-quantile value of duration, $q_D(0.5) = 3$ (days) and similarly $q_D(0.75) = 7$ (days) and $q_D(0.9) = 19$ (days). To understand the spatial pattern, the

Table 1
The values of duration (D), volume (V) and peak (Q) at 50th-quantile (median), 75th-quantile (moderate), and 90th-quanitle (extreme) for the entire country.

	50th-quantile	75th-quantile	90th-quantile
Duration (D) (days)	3	7	19
Volume (V)	0.426	2.014	8.839
Peak (Q)	0.277	0.628	1.139

quantile values at each gridded cell were also computed shown in Fig. 7. The findings reveal that the extreme values of duration and volume occur in the west and south regions are higher than those in other areas.

The joint exceedance probabilities of duration, volume and peak in different combination scenarios are presented in Figs. 8–10. The interpretation of those figures is straightforward where the results show a remarkable difference in the spatial pattern of the exceedance probability. In Fig. 8, at 50th-quantile (q(0.5)), the chance that a flood event with $D \geq q(0.5) = 3$ (days), $V \geq q(0.5) = 0.426$, and $Q \geq q(0.5) = 0.277$ co-occurrence is about 60–70% in the regions along the administrative borders of Chin, Sagaing, Mandalay, Shan, Nay Pyi Taw, and Keyan while this probability is slightly lower, about 40–50%, at Ayeyarwadi, Bago, Yangon, Kayin and a major part of Kachin. In the case when $D \geq q(0.5)$ and $Q \geq q(0.5)$, the probability that $V \geq q(0.9)$ (extreme) at the same time ranges from 10 to 30%, except for the north (Kachin) and east (Shan). In addition, the probability that duration exceeds the median, i.e. $D \geq q(0.5) = 3$ (days), and volume and peak exceed the extreme, i.e. $V \geq q(0.9) = 8.839$ and $Q \geq q(0.9) = 1.139$, is about 10–20% in Chin and southwest of Sagaing, Nay Pyi Taw and regions around its border, south of Kayin, Mon, and from north to east of Tanintharyi. The

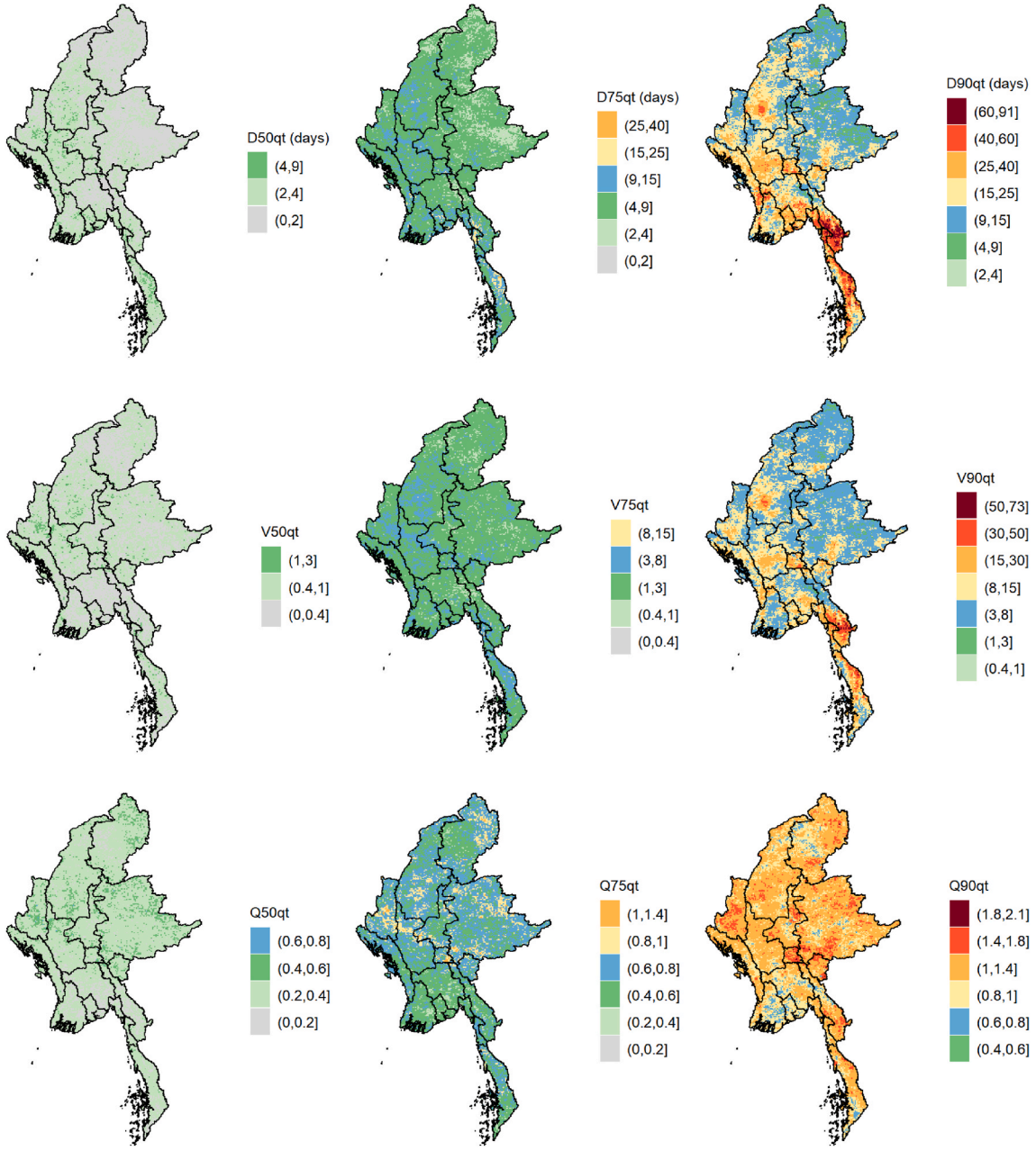

Fig. 7. The values of duration (D) (top), volume (V) (middle) and peak (Q) (bottom) at 50th-quantile (50qt) (median), 75th-quantile (75qt) (moderate), and 90th-quantile (90qt) (extreme).

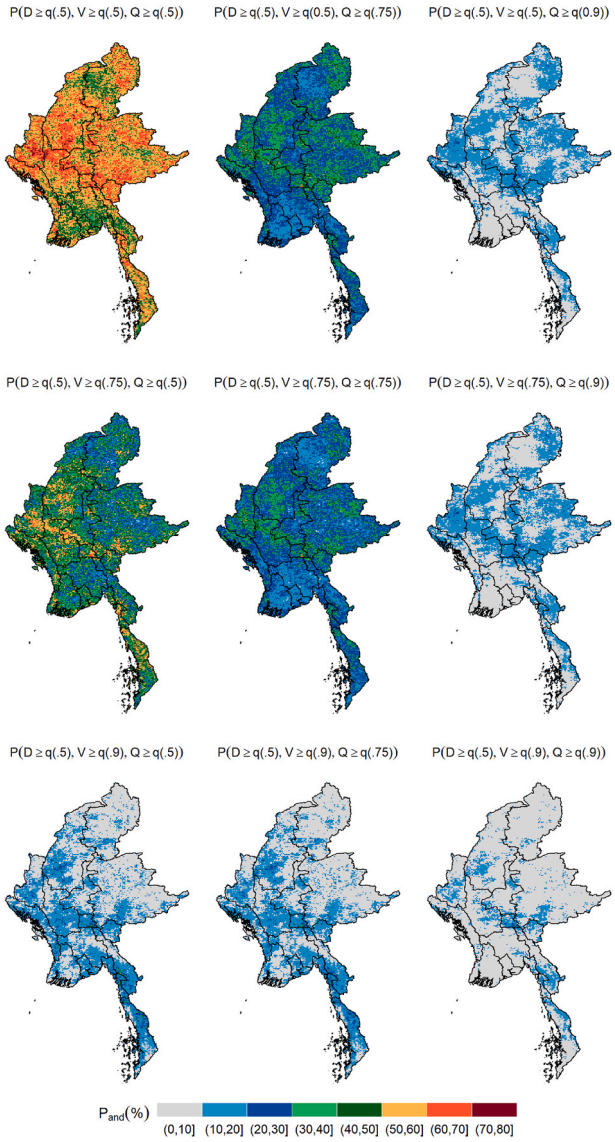

Fig. 8. Probabilities of duration (D), volume (V), and peak (Q) exceeding thresholds simultaneously where different scenarios of thresholds of D being greater than or equal to 50th-quantile (median) are combined with V and Q being greater than or equal to 50th-quantile (median), 75th-quantile (moderate), and 90th-quanitle (extreme). The quantile values were computed for the entire country.

probability of such a scenario occurring is less than 10% in the remaining parts of the country.

Similar probabilistic risk analysis performed, however, when duration exceeding 75th-quantile (moderate) and 90th-quantile (extreme) combined with different scenarios of volume and peak are presented in Figs. 9 and 10, respectively. In Fig. 9, the probability of $D \geq q(0.75) = 7$ (days), $V \geq q(0.5) = 0.426$, and $Q \geq q(0.5) = 0.277$ is 40–60% majorly occurred in Sagaing, Magway, Rakhine, Mon and Tanintharyi and up to 60–70% in some regions such as south of Shan, Chin, and Nay Pyi Taw.

In general, when $D \geq q(0.75)$, the probability that volume or duration or both exceed the extreme (90th-quantile) is less than 20%. Fig. 10 highlights the high risk region of occurring extreme duration, i.e. $D \geq q(0.9) = 19$ (days) including southwest of Sagaing, south of Magway, Bago and Kayin, Rakhine, Yangon, Mon, and Tanintharyi. In the worst case, the probability that all duration, volume, and peak exceed the extreme values, i.e. $D \geq q(0.9)$, $V \geq q(0.9)$, and $Q \geq q(0.9)$, is about 10–15% in regions such as southwest of Sagaing, southeast of Chin, Nay Pyi Taw, Mon and areas around these states. The highest risk area with the probability up to 30%, which exceeds extreme duration, volume, and peak simultaneously is southeast of Dekkhinathiri township (Nay Pyi Taw).

3.2. SAPI evaluation

Here, we tested how the SAPI derived from CHIRPS agrees with SAPI based on ground observations. We interrogated two data sources including Global Historical Climatology Network Daily (GHCND) and Global Surface Summary of the Day (GSOD). Both

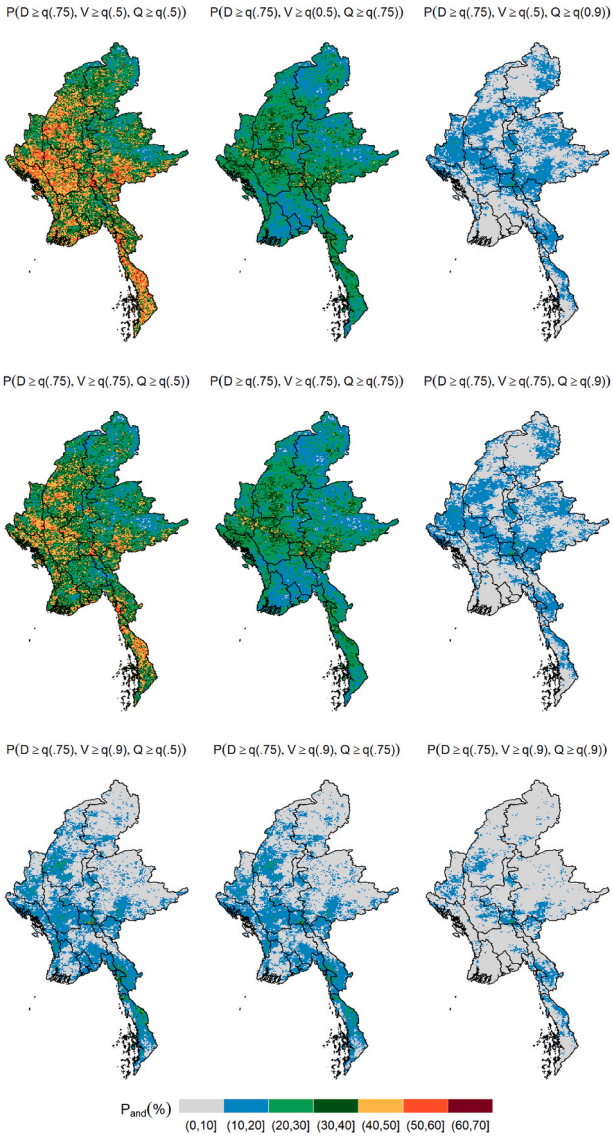

Fig. 9. Probabilities of duration (D), volume (V), and peak (Q) exceeding thresholds simultaneously where different scenarios of thresholds of D being greater than or equal to 75th-quantile (moderate) are combined with V and Q being greater than or equal to 50th-quantile (median), 75th-quantile (moderate), and 90th-quanitle (extreme). The quantile values were computed for the entire country.

datasets have daily precipitation summaries provided by National Centers for Environmental Information (NOAA). Over Myanmar, GHCND and GSOD have five (Fig. 1) and twenty-four stations, respectively. Both datasets are extremely patchy; however, the GHCND data is better (see Fig. S4 in Supplementary) and thus only GHCND data was used for validation (GSOD data are not shown here). For the purpose of SAPI computation requiring daily data and a long climatology period, and also matching with CHIRPS data (1981–2019), the missing values in GHCND time series were imputed by values from CHIRPS.

Fig. 11 represents the percent consistent (PC) (Charles et al., 2015) of the events, when SAPI >0, derived from CHIRPS and GHCND datasets. The PC is formulated as:

$$PC = \frac{total\ events\ when\ SAPI > 0\ at\ the\ same\ time\ in\ both\ CHIRPS\ and\ GHCND}{total\ events\ when\ SAPI > 0\ in\ GHCND} \tag{14}$$

The PC values vary across five stations, Myitkyina (57%), Mandalay (33%), Sittwe (86%), Yangon Intl (80%), and Victoria Point (95%). It is noted that the results were highly affected by the missing values from ground-based observations and hence should be interpreted with care. Fig. 1 (b) also shows an example of the SAPI time series for Bilin town (17.225° N, 97.225° E) in Mon state, Myanmar from July 1, 2019 to October 31, 2019. It is worth pointing out that the onset date, i.e., when SAPI starts being above zero, was August 6, 2019. According to the Department of Meteorology and Hydrology of Myanmar, the observed water level condition of Bilin river at Bilin reached the danger level on August 7, 2019 (Fig. S5 in Supplementary).

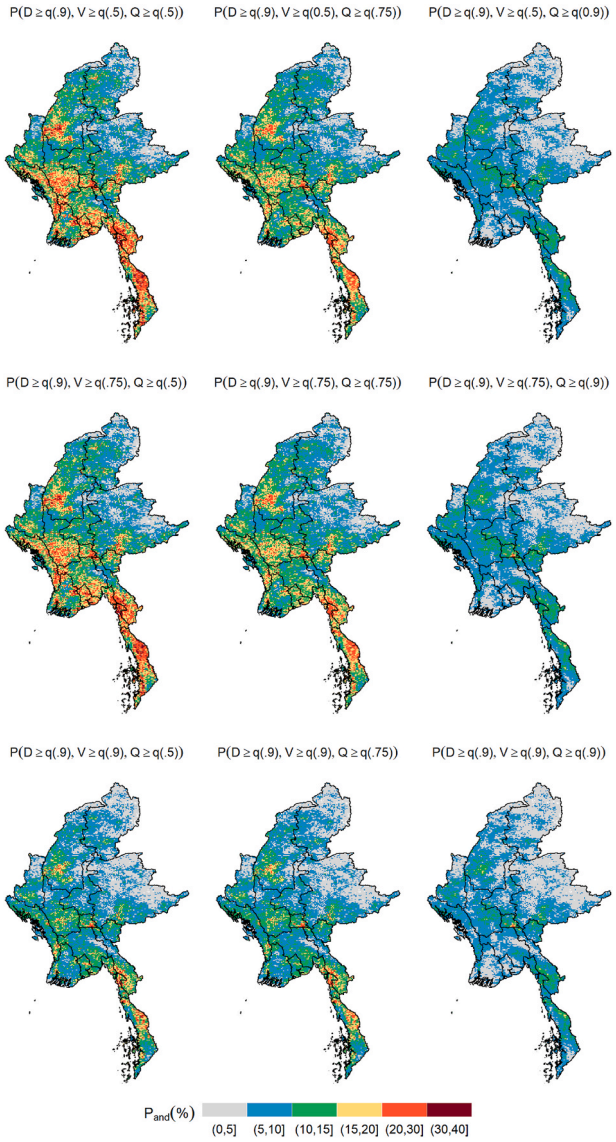

Fig. 10. Probabilities of duration (D), volume (V), and peak (Q) exceeding thresholds simultaneously where different scenarios of thresholds of D being greater than or equal to 90th-quantile (extreme) are combined with V and Q being greater than or equal to 50th-quantile (median), 75th-quantile (moderate), and 90th-quanitle (extreme). The quantile values were computed for the entire country.

4. Discussion

Given the stochastic nature of rainfall, and many of the processes that contribute to flooding, a probabilistic based framework that has simultaneously different characteristics (i.e., duration, volume and peak) is required to more accurately assess risk. Thus, the main motivation of the present study is to demonstrate how remotely sensed data and copula statistical methods can be applied to assess and map flood risks over large areas where station data is lacking. In addition, we show the potential flexibility and efficiency of the multivariate copula model in modelling the flood characteristics, particularly when dependence between variables is complex and the data contains outliers, i.e., extreme values. Examples of methodological papers investing flood characteristics are published by Jeong et al. (2014) Daneshkhah et al. (2016), Latif and Mustafa (2020b), Latif and Mustafa (2020a), Latif and Mustafa (2020c). As a result, the aim of this study is not to deliver an ultimate model of extreme flood events which generally requires more input information such as land use and land cover, elevation, slope, river network, and drainage system to be integrated into the model. Instead, we developed a satellite-based antecedence precipitation index that can be used as an indicator of flood events and quantified the joint exceedance probability of flood characteristics including duration, volume, and peak.

Another motivation of the methodology developed in our paper is to model the joint distribution of flood characteristics in a probabilistic way and particularly to provide a framework for the cases when data is limited, or no data is available. The case of data limitation is very common in extreme value theory and risk analysis, and hence the copula-based method is effective and efficient when

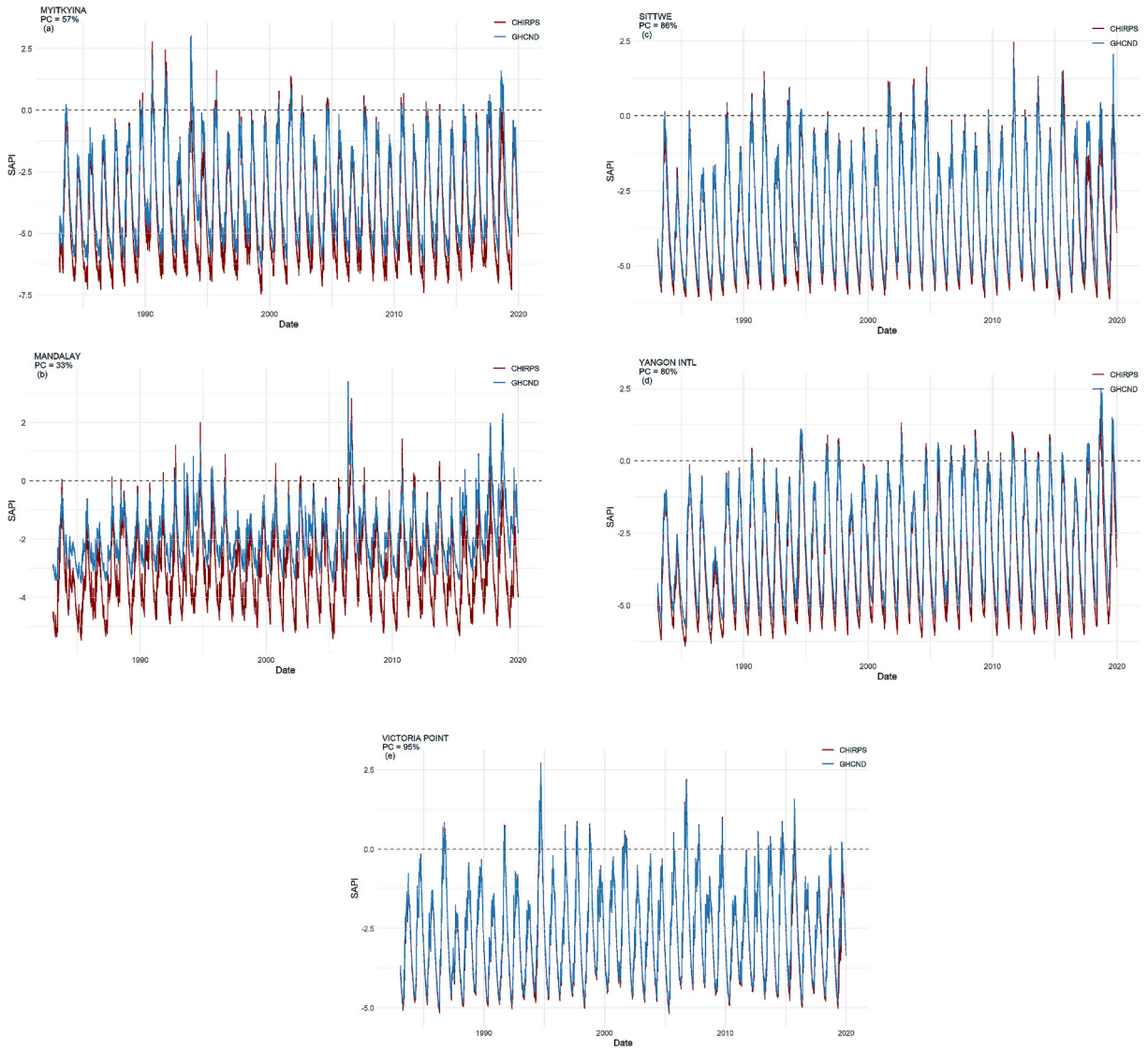

Fig. 11. Daily Standardized Antecedent Precipitation Index (SAPI) derived from daily precipitation (mm) extracted from Climate Hazards Group InfraRed Precipitation with Station data (CHIRPS) and Global Historical Climatology Network daily (GHCND) at five stations in Myanmar for the period of February 01, 1982–December 31, 2019 (38 years). Percent consistent (PC) refers to the percentage of the total events when SAPI >0 that are consistent between two datasets over the total events based on ground-based GHCND datasets.

used for approximating modelling when data is limited. When data is not available, the copula-based method can be used for synthetic data generation for machine learning emulators in weather and climate (see Hong et al. (2016) and Meyer et al. (2021) for further details).

A limitation of this study is that there is very limited observed data available from Myanmar for the validation of the proposed index. This problem has been also mentioned by previous studies (Taft and Evers 2016; Phongsapan et al., 2019). Therefore, validating the proposed antecedence precipitation index against observations over the study area is highly recommended. Future research including other flood prediction methods and analysis techniques such as trend analysis and breakpoint analysis will improve analysis and assessment of flood risk. Also, when the spatiotemporally dense flood maps derived from satellite data are integrated with data from secondary sources on historical flood impacts, it is possible to classify regions into flood zones with homogeneous characteristics based on different levels of risk. For example, Khaing et al. (2019) applied MODIS flood inundation images in conjunction with other datasets such as topography and land cover to derive flood hazard maps or simulate the spatial extent of flooding.

The satellite-based antecedence precipitation index (SAPI) and probabilistic framework proposed in this study are also useful for other research and practical applications. For example, as indicated by several recent studies, flood characteristics (peak discharge, duration, and volume) exhibit nonstationary behaviour due to changes in land use and land cover, urbanization, climate, and water resource structures (Liu et al., 2017; Dong et al., 2019). As a result, the assumption of temporal stationarity in flood characteristics is

not always valid and potentially leads to an underestimation of flood risk. Thus, it is possible to perform multivariate frequency analysis of extreme discharge events in a nonstationary condition by modelling parameters of marginal distributions with covariates, such as antecedent precipitation.

Furthermore, the present framework is applicable for practical projects of hydrological works, where the joint probability of flood characteristics can be used for different design events. Examples include design events derived from different bivariate and multivariate conditional probabilities and return periods as considered in Salvadori et al. (2011) and Gräler et al. (2013). The satellite-based antecedence precipitation index was developed for flood detection and risk analysis, however, because of its characteristics, the index can also be used as a tool to monitor drier-than-normal conditions, for example, the study of Malik et al. (2020).

Another important application of the proposed satellite-based standardized antecedence precipitation index is in the context of index-based insurance. Index-based insurance does not suffer common problems of moral hazard and adverse selection as in conventional insurance (Adeyinka et al., 2022). Instead, index insurance triggers payouts based on external indicators. However, index-based insurance often uses ground-based indicators such as weather and area yield, which rely on historical data for the design, pricing, and calibration of products. The data have to meet commercial insurer and re-insurer requirements such as long historical data with only a small percentage of missing or out-of-range values of the total datasets, the distance between weather stations and insured farms, secure and trustworthy data recording. These requirements make the operation of ground-based index-based insurance products in rural areas difficult since the weather stations are often very scattered. Thus, index-based insurance using indices or indicators derived from satellite data, such as the standardized antecedence precipitation index in this study, can offer many advantages. Remotely sensed data are spatially continuous across large areas of the earth, available in near real-time, can be freely accessible and available, have extended historical records, and are difficult to influence by either the insured or insurer.

Finally, many operational satellite-based precipitation products (SPPs) have recently become available with quasi-global coverage and at sub-daily temporal resolution. SPPs provide important information for hydrological applications (e.g., flood or flash flood analysis) in sparsely gauged or ungauged basins (Jiang et al., 2018; Yuan et al., 2018; Liu et al., 2019). For example, Yuan et al. (2019) used the precipitation products from Tropical Rainfall Measuring Mission (TRMM) and Global Precipitation Measurement (GPM) for flood simulations at sub-daily scales in a poorly gauged watershed in Myanmar. The results indicated that the SPPs (3B42RT) acquired from TRMM Multi-satellite Precipitation Analysis were suitable for hydrological performance in a 3-hourly flood simulation. Maggioni and Massari (2018) reviewed the performance of SPPs in riverine flood modeling and concluded that the use of satellite data in flood forecasting is significantly promising. However, Maggioni and Massari (2018) argue that for operational purposes the maturity of SPP-forced models is currently insufficient. Therefore, further research on bias correction methods of different complexity and characteristics of the region, such as population density, land use, geophysical and climate is needed to improve the performance of current hydrologic models used to predict floods.

5. Conclusion

This study developed a probabilistic framework of multivariate frequency analysis that takes into account the advantages of advanced high resolution remotely sensed data (CHIRPS) and statistical copula-based techniques for Myanmar. A standardized antecedence precipitation index (SAPI) that can be used as a flood indicator and its associated characteristics including duration, volume, and peak was developed from satellite-derived precipitation using a time-dependent reduction function. Vine copulas were applied to model the joint distribution between event characteristics to derive important information of the exceedance probability for flood risk analysis and assessment. The southwest and south regions are found to be at high risk from floods (as indicated by the characteristics SAPI) in the rainy monsoon season, i.e., in August and September. The results also show a strong relationship among duration, volume, and peak of an extreme event. In addition, the results reveal a significant difference in spatial patterns of the joint exceedance probability of event characteristics in different scenario combinations. The proposed approach is applicable to improve risk assessment and potentially useful in different hydrological design events and the context of index-based insurance.

Author statement

Thong Nguyen-Huy: Conceptualization, Methodology, Software, Validation, Formal analysis, Data Curation, Writing - Original Draft, Writing - Review & Editing, Visualization. **Jarrod Kath:** Conceptualization, Software, Formal analysis, Writing - Review & Editing. **Thomas Nagler:** Methodology, Software, Writing - Review & Editing. **Ye Khaung**: Data Curation, Writing - Review & Editing. **Thee Su Su Aung:** Data Curation, Writing - Review & Editing. **Shahbaz Mushtaq:** Conceptualization, Formal analysis, Writing - Original Draft, Writing - Review & Editing, Supervision, Project administration. **Torben Marcussen:** Formal analysis**,** Data Curation, Writing - Review & Editing. **Roger Stone:** Supervision, Project administration, Funding acquisition.

Ethical Statement for Solid State Ionics

Hereby, I/insert author name/consciously assure that for the manuscript/insert title/the following is fulfilled:

1) This material is the authors' own original work, which has not been previously published elsewhere.
2) The paper is not currently being considered for publication elsewhere.
3) The paper reflects the authors' own research and analysis in a truthful and complete manner.
4) The paper properly credits the meaningful contributions of co-authors and co-researchers.
5) The results are appropriately placed in the context of prior and existing research.

6) All sources used are properly disclosed (correct citation). Literally copying of text must be indicated as such by using quotation marks and giving proper reference.
7) All authors have been personally and actively involved in substantial work leading to the paper, and will take public responsibility for its content.

The violation of the Ethical Statement rules may result in severe consequences.

To verify originality, your article may be checked by the originality detection software iThenticate. See also http://www.elsevier.com/editors/plagdetect.

I agree with the above statements and declare that this submission follows the policies of Solid State Ionics as outlined in the Guide for Authors and in the Ethical Statement.

Declaration of competing interest

The authors declare that they have no known competing financial interests or personal relationships that could have appeared to influence the work reported in this paper.

Acknowledgement

This work was funded by the German Federal Ministry for the Environment, Nature Conservation and Nuclear Safety through the International Climate Initiative and partially supported by a Spinoza grant awarded by the Netherlands Organisation of Scientific Research (NWO). We would like to thank the National Centers for Environmental Information (NOAA) for publishing the Global Historical Climatology Network Daily (GHCND) and Global Surface Summary of the Day (GSOD) datasets. We especially thank anonymous reviewers for their suggestions and comments.

Appendix A. Supplementary data

Supplementary data to this article can be found online at https://doi.org/10.1016/j.rsase.2022.100733.

References

Aas, K., Czado, C., Frigessi, A., Bakken, H., 2009. Pair-copula constructions of multiple dependence. Insur. Math. Econ. 44 (2), 182–198.
Acierto, R.A.E., Kawasaki, A., Zin, W.W., 2020. Impact of bias-correction methods in assessing the potential flood frequency change in the Bago river. J. Disaster Res. 15 (3), 288–299.
Adeyinka, A.A., Kath, J., Nguyen-Huy, T., Mushtaq, S., Souvignet, M., Range, M., Barratt, J., 2022. Global disparities in agricultural climate index-based insurance research. Climate Risk Manag., 100394
ADPC, 2009. Institutional Arrangements for Disaster Management in Myanmar. Asian Disaster Preparedness Center. https://www.preventionweb.net/files/14637_14637Binding1.pdf.
Ali, M., Deo, R.C., Downs, N.J., Maraseni, T., 2018. Multi-stage hybridized online sequential extreme learning machine integrated with Markov chain Monte Carlo copula-Bat algorithm for rainfall forecasting. Atmos. Res. 213, 450–464.
Bai, L., Shi, C., Li, L., Yang, Y., Wu, J., 2018. Accuracy of CHIRPS satellite-rainfall products over mainland China. Rem. Sens. 10 (3), 362.
Bedford, T., Cooke, R.M., 2002. Vines: a new graphical model for dependent random variables. Ann. Stat. 1031–1068.
Byun, H.-R., Lee, D.-K., 2002. Defining three rainy seasons and the hydrological summer monsoon in Korea using available water resources index. J. Meteorol. Soc. Japan. Ser. II 80 (1), 33–44.
Cavalcante, R.B.L., da Silva Ferreira, D.B., Pontes, P.R.M., Tedeschi, R.G., da Costa, C.P.W., de Souza, E.B., 2020. Evaluation of extreme rainfall indices from CHIRPS precipitation estimates over the Brazilian Amazonia. Atmos. Res. 238, 104879.
Charles, A.N., Duell, R.E., Wang, X., Watkins, A.B., 2015. Seasonal forecasting for Australia using a dynamical model: improvements in forecast skill over the operational statistical model. Australian Meteorol. Oceanographic J. 65 (3), 356–375.
Chebana, F., Ouarda, T.B., 2009. Index flood–based multivariate regional frequency analysis. Water Resour. Res. 45 (10).
Chebana, F., Ouarda, T.B., 2011. Multivariate quantiles in hydrological frequency analysis. Environmetrics 22 (1), 63–78.
Cian, F., Marconcini, M., Ceccato, P., 2018. Normalized Difference Flood Index for rapid flood mapping: taking advantage of EO big data. Remote Sens. Environ. 209, 712–730.
Czado, C., 2019. 'Analyzing Dependent Data with Vine Copulas', Lecture Notes in Statistics. Springer.
Daneshkhah, A., Remesan, R., Chatrabgoun, O., Holman, I.P., 2016. Probabilistic modeling of flood characterizations with parametric and minimum information pair-copula model. J. Hydrol. 540, 469–487.
de Melo Mendes, B.V., Semeraro, M.M., Leal, R.P.C., 2010. 'Pair-copulas modeling in finance. Financ. Mark. Portfolio Manag. 24 (2), 193–213.
Deo, R.C., Byun, H.-R., Adamowski, J.F., Kim, D.-W., 2015. A real-time flood monitoring index based on daily effective precipitation and its application to Brisbane and Lockyer Valley flood events. Water Resour. Manag. 29 (11), 4075–4093.
Deo, R.C., Byun, H.-R., Kim, G.-B., Adamowski, J.F., 2018. A real-time hourly water index for flood risk monitoring: pilot studies in Brisbane, Australia, and Dobong Observatory, South Korea. Environ. Monit. Assess. 190 (8), 1–27.
Dinku, T., Funk, C., Peterson, P., Maidment, R., Tadesse, T., Gadain, H., Ceccato, P., 2018. Validation of the CHIRPS satellite rainfall estimates over eastern Africa. Q. J. R. Meteorol. Soc. 144, 292–312.
Dong, N.D., Agilan, V., Jayakumar, K., 2019. Bivariate flood frequency analysis of nonstationary flood characteristics. J. Hydrol. Eng. 24 (4), 4019007.
Dutta, R., 2018. Drought monitoring in the dry zone of Myanmar using MODIS derived NDVI and satellite derived CHIRPS precipitation data. Sustain. Agric. Res. 7 (526–2020-473), 46–55.
Favre, A.C., El Adlouni, S., Perreault, L., Thiémonge, N., Bobée, B., 2004. Multivariate hydrological frequency analysis using copulas. Water Resour. Res. 40 (1).
FloodList, 2019. Myanmar – More Flooding as Rivers Rise in Ayeyarwady, Mon and Kayin viewed 23 July. https://floodlist.com/asia/myanmar-flood-rivers-ayeyarwady-mon-kayin-august-2019.
Funk, C., Peterson, P., Landsfeld, M., Pedreros, D., Verdin, J., Shukla, S., Husak, G., Rowland, J., Harrison, L., Hoell, A., Michaelsen, J., 2015. The climate hazards infrared precipitation with stations—a new environmental record for monitoring extremes. Sci. Data 2 (1), 150066.

Ganaie, H.A., Hashaia, H., Kalota, D., 2013. Delineation of flood prone area using Normalized Difference Water Index (NDWI) and transect method: a case study of Kashmir Valley. Int. J. Remote Sens. Appl 3 (2), 53–58.
Gao, F., Zhang, Y., Ren, X., Yao, Y., Hao, Z., Cai, W., 2018. Evaluation of CHIRPS and its application for drought monitoring over the Haihe river basin, China. Nat. Hazards 92 (1), 155–172.
Gräler, B., Van Den Berg, M., Vandenberghe, S., Petroselli, A., Grimaldi, S., Baets, Bd, Verhoest, N., 2013. Multivariate return periods in hydrology: a critical and practical review focusing on synthetic design hydrograph estimation. Hydrol. Earth Syst. Sci. 17 (4), 1281–1296.
Gupta, V., Jain, M.K., Singh, P.K., Singh, V., 2020. An assessment of global satellite-based precipitation datasets in capturing precipitation extremes: a comparison with observed precipitation dataset in India. Int. J. Climatol. 40 (8), 3667–3688.
Hallegatte, S., Green, C., Nicholls, R.J., Corfee-Morlot, J., 2013. Future flood losses in major coastal cities. Nat. Clim. Change 3 (9), 802–806.
Hong, N.-M., Lee, T.-Y., Chen, Y.-J., 2016. Daily weather generator with drought properties by copulas and standardized precipitation indices. Environ. Monit. Assess. 188 (6), 1–14.
Jaworski, P., Durante, F., Härdle, W.K., 2013. Copulae in Mathematical and Quantitative Finance', *Lecture Notes in Statistics-Proceedings*. Springer, Heidelberg.
Jeong, D.I., Sushama, L., Khaliq, M.N., Roy, R., 2014. A copula-based multivariate analysis of Canadian RCM projected changes to flood characteristics for northeastern Canada. Clim. Dynam. 42 (7–8), 2045–2066.
Ji, L., Zhang, L., Wylie, B., 2009. Analysis of dynamic thresholds for the normalized difference water index. Photogramm. Eng. Rem. Sens. 75 (11), 1307–1317.
Jiang, S., Ren, L., Xu, C.-Y., Yong, B., Yuan, F., Liu, Y., Yang, X., Zeng, X., 2018. Statistical and hydrological evaluation of the latest Integrated Multi-satellitE Retrievals for GPM (IMERG) over a midlatitude humid basin in South China. Atmos. Res. 214, 418–429.
Joe, H., 1996. Families of m-Variate Distributions with Given Margins and m (m-1)/2 Bivariate Dependence Parameters. Lecture Notes-Monograph Series, pp. 120–141.
Karmakar, S., Simonovic, S., 2008. Bivariate flood frequency analysis: Part 1. Determination of marginals by parametric and nonparametric techniques. J. Flood Risk Manag. 1 (4), 190–200.
Karmakar, S., Simonovic, S., 2009. Bivariate flood frequency analysis. Part 2: a copula-based approach with mixed marginal distributions. J. Flood Risk Manag. 2 (1), 32–44.
Khaing, Z.M., Zhang, K., Sawano, H., Shrestha, B.B., Sayama, T., Nakamura, K., 2019. 'Flood hazard mapping and assessment in data-scarce Nyaungdon area, Myanmar'. PLoS One 14 (11), e0224558.
Kyaw, K.K., Lolupiman, T., Thanathanphon, W., Sisomphon, P., 2020. Validation of satellite datasets for the operation of flood and drought indicators in certain regions of Myanmar. In: Proceedings of the 22nd IAHR-APD Congress 2020, Sapporo, Japan.
Latif, S., Mustafa, F., 2020a. Parametric vine copula construction for flood analysis for Kelantan river basin in Malaysia. Civ. Eng. J. 6 (8), 1470–1491.
Latif, S., Mustafa, F., 2020b. Bivariate joint distribution analysis of the flood characteristics under semiparametric copula distribution framework for the Kelantan River basin in Malaysia. J. Ocean Eng. Sci.
Latif, S., Mustafa, F., 2020c. Trivariate distribution modelling of flood characteristics using copula function—a case study for Kelantan River basin in Malaysia. AIMS Geosciences 6 (1), 92–130.
Le, M.-H., Lakshmi, V., Bolten, J., Du Bui, D., 2020. Adequacy of satellite-derived precipitation estimate for hydrological modeling in Vietnam Basins. J. Hydrol. 586, 124820.
Liu, J., Zhang, Q., Singh, V.P., Gu, X., Shi, P., 2017. Nonstationarity and clustering of flood characteristics and relations with the climate indices in the Poyang Lake basin, China. Hydrol. Sci. J. 62 (11), 1809–1824.
Liu, S., Hu, K., Zhang, S., Zeng, Y., 2019. Comprehensive evaluation of satellite-based precipitation at sub-daily time scales over a high-profile watershed with complex terrain. Earth Space Sci. 6 (12), 2347–2361.
Luo, X., Wu, W., He, D., Li, Y., Ji, X., 2019. Hydrological simulation using TRMM and CHIRPS precipitation estimates in the lower Lancang-Mekong river basin. Chin. Geogr. Sci. 29 (1), 13–25.
MacLeod, D., Easton-Calabria, E., de Perez, E.C., Jaime, C., 2021. Verification of forecasts for extreme rainfall, tropical cyclones, flood and storm surge over Myanmar and the Philippines. Weather Clim. Extrem. 33, 100325.
Maggioni, V., Massari, C., 2018. On the performance of satellite precipitation products in riverine flood modeling: a review. J. Hydrol. 558, 214–224.
Malik, A., Kumar, A., Kisi, O., Khan, N., Salih, S.Q., Yaseen, Z.M., 2020. 'Analysis of dry and wet climate characteristics at Uttarakhand (India) using effective drought index'. Nat. Hazards 1–20.
McFeeters, S.K., 1996. The use of the Normalized Difference Water Index (NDWI) in the delineation of open water features. Int. J. Rem. Sens. 17 (7), 1425–1432.
McKee, T.B., Doesken, N.J., Kleist, J., 1993. The relationship of drought frequency and duration to time scales. In: Proceedings of the 8th Conference on Applied Climatology, Boston, pp. 179–183.
Memon, A.A., Muhammad, S., Rahman, S., Haq, M., 2015. Flood monitoring and damage assessment using water indices: a case study of Pakistan flood-2012. Egyptian J. Remote Sens. Space Sci. 18 (1), 99–106.
Meyer, D., Nagler, T., Hogan, R.J., 2021. 'Copula-based synthetic data generation for machine learning emulators in weather and climate: application to a simple radiation model'. Geosci. Model Dev. Discuss. (GMDD) 1–21.
Mirabbasi, R., Fakheri-Fard, A., Dinpashoh, Y., 2012. Bivariate drought frequency analysis using the copula method. Theor. Appl. Climatol. 108 (1), 191–206.
Nagler, T., 2018a. A generic approach to nonparametric function estimation with mixed data. Stat. Probab. Lett. 137, 326–330.
Nagler, T., 2018b. Asymptotic analysis of the jittering kernel density estimator. Math. Methods Stat. 27 (1), 32–46.
Nagler, T., Czado, C., 2016. Evading the curse of dimensionality in nonparametric density estimation with simplified vine copulas. J. Multivariate Anal. 151, 69–89.
Nagler, T., Vatter, T., 2018a. rvinecopulib: high performance algorithms for vine copula modeling. R package version 2 (5).
Nagler, T., Vatter, T., 2018b. Kde1d: Univariate Kernel Density Estimation', R Package Version 0.3. 0.
Nagler, T., Schellhase, C., Czado, C., 2017. Nonparametric estimation of simplified vine copula models: comparison of methods. Depend. Model. 5 (1), 99–120.
Nguyen-Huy, T., Deo, R.C., Mushtaq, S., Khan, S., 2020a. Probabilistic seasonal rainfall forecasts using semiparametric d-vine copula-based quantile regression. In: Handbook of Probabilistic Models. Elsevier, pp. 203–227.
Nguyen-Huy, T., Deo, R.C., Mushtaq, S., Kath, J., Khan, S., 2018. Copula-based agricultural conditional value-at-risk modelling for geographical diversifications in wheat farming portfolio management. Weather Clim. Extrem. 21, 76–89.
Nguyen-Huy, T., Deo, R.C., Mushtaq, S., Kath, J., Khan, S., 2019. Copula Statistical Models for Analyzing Stochastic Dependencies of Systemic Drought Risk and Potential Adaptation Strategies. Stochastic Environmental Research and Risk Assessment.
Nguyen-Huy, T., Deo, R.C., Yaseen, Z.M., Prasad, R., Mushtaq, S., 2020b. Bayesian Markov chain Monte Carlo-based copulas: factoring the role of large-scale climate indices in monthly flood prediction. In: Intelligent Data Analytics for Decision-Support Systems in Hazard Mitigation. Springer, pp. 29–47.
Nguyen-Huy, T., Kath, J., Mushtaq, S., Cobon, D., Stone, G., Stone, R., 2020c. Integrating El Niño-Southern Oscillation information and spatial diversification to minimize risk and maximize profit for Australian grazing enterprises. Agron. Sustain. Dev. 40 (1), 4.
OECD, 2016. Financial Management of Flood Risk.
Paredes-Trejo, F.J., Barbosa, H., Kumar, T.L., 2017. Validating CHIRPS-based satellite precipitation estimates in Northeast Brazil. J. Arid Environ. 139, 26–40.
Perdigón-Morales, J., Romero-Centeno, R., Pérez, P.O., Barrett, B.S., 2018. The midsummer drought in Mexico: perspectives on duration and intensity from the CHIRPS precipitation database. Int. J. Climatol. 38 (5), 2174–2186.
Phongsapan, K., Chishtie, F., Poortinga, A., Bhandari, B., Meechaiya, C., Kunlamai, T., Aung, K.S., Saah, D., Anderson, E., Markert, K., 2019. Operational flood risk index mapping for disaster risk reduction using Earth Observations and cloud computing technologies: a case study on Myanmar. Front. Environ. Sci. 191.
Prasad, R., Charan, D., Joseph, L., Nguyen-Huy, T., Deo, R.C., Singh, S., 2020. Daily flood forecasts with intelligent data analytic models: multivariate empirical mode decomposition-based modeling methods. In: Intelligent Data Analytics for Decision-Support Systems in Hazard Mitigation. Springer, pp. 359–381.
Reddy, M.J., Ganguli, P., 2012. Bivariate flood frequency analysis of Upper Godavari River flows using Archimedean copulas. Water Resour. Manag. 26 (14), 3995–4018.

Rivera, J.A., Marianetti, G., Hinrichs, S., 2018. Validation of CHIRPS precipitation dataset along the central andes of Argentina. Atmos. Res. 213, 437–449.
Rogers, A., Kearney, M., 2004. Reducing signature variability in unmixing coastal marsh Thematic Mapper scenes using spectral indices. Int. J. Rem. Sens. 25 (12), 2317–2335.
Saghafian, B., Mehdikhani, H., 2014. Drought characterization using a new copula-based trivariate approach. Nat. Hazards 72 (3), 1391–1407.
Salvadori, G., Michele, C.D., Durante, F., 2011. On the return period and design in a multivariate framework. Hydrol. Earth Syst. Sci. 15 (11), 3293–3305.
Seiler, R., Hayes, M., Bressan, L., 2002. Using the standardized precipitation index for flood risk monitoring. Int. J. Climatol.: J. Royal Meteorol. Soc. 22 (11), 1365–1376.
Shafaei, M., Fakheri-Fard, A., Dinpashoh, Y., Mirabbasi, R., De Michele, C., 2017. Modeling flood event characteristics using D-vine structures. Theor. Appl. Climatol. 130 (3–4), 713–724.
Shen, Z., Yong, B., Gourley, J.J., Qi, W., Lu, D., Liu, J., Ren, L., Hong, Y., Zhang, J., 2020. Recent global performance of the climate hazards group infrared precipitation (CHIRP) with stations (CHIRPS). J. Hydrol. 591, 125284.
Shiau, J., 2003. Return period of bivariate distributed extreme hydrological events. Stoch. Environ. Res. Risk Assess. 17 (1), 42–57.
Shiau, J., 2006. Fitting drought duration and severity with two-dimensional copulas. Water Resour. Manag. 20 (5), 795–815.
Shiau, J.T., Wang, H.Y., Tsai, C.T., 2006. Bivariate frequency analysis of floods using copulas1. JAWRA J. Am. Water Resour. Assoc. 42 (6), 1549–1564.
Sklar, M., 1959. Fonctions de répartition à n dimensions et leurs marges. Université Paris 8.
Taft, L., Evers, M., 2016. A review of current and possible future human–water dynamics in Myanmar's river basins. Hydrol. Earth Syst. Sci. 20 (12), 4913–4928.
Tosunoglu, F., Gürbüz, F., İspirli, M.N., 2020. Multivariate modeling of flood characteristics using Vine copulas. Environ. Earth Sci. 79 (19), 1–21.
UoM, 2009. Hazard Profile of Myanmar. Union of Myanmar (Department of Meteorology and Hydrology (DMH), Forest Department, Relief and Resettlement Department, Irrigation Department and Fire Services Department), Myanmar Engineering Society (MES), Myanmar Geosciences Society (MGS), Myanmar Information Management Unit (MIMU) and Asian Disaster Preparedness Center (ADPC). http://www.ssstj.sci.ssru.ac.th/Content/journals/Volume3_No1/SSSTJ_Volume3_No1_January_2016.pdf#page=22.
Vergni, L., Todisco, F., Mannocchi, F., 2015. Analysis of agricultural drought characteristics through a two-dimensional copula. Water Resour. Manag. 29 (8), 2819–2835.
Xiao, X., Hollinger, D., Aber, J., Goltz, M., Davidson, E.A., Zhang, Q., Moore III, B., 2004. Satellite-based modeling of gross primary production in an evergreen needleleaf forest. Remote Sens. Environ. 89 (4), 519–534.
Yevjevich, V.M., 1967. Objective Approach to Definitions and Investigations of Continental Hydrologic Droughts. An', Colorado State University, Libraries.
Yuan, F., Zhang, L., Soe, K.M.W., Ren, L., Zhao, C., Zhu, Y., Jiang, S., Liu, Y., 2019. Applications of TRMM-and GPM-era multiple-satellite precipitation products for flood simulations at sub-daily scales in a sparsely gauged watershed in Myanmar. Rem. Sens. 11 (2), 140.
Yuan, F., Wang, B., Shi, C., Cui, W., Zhao, C., Liu, Y., Ren, L., Zhang, L., Zhu, Y., Chen, T., 2018. Evaluation of hydrological utility of IMERG Final run V05 and TMPA 3B42V7 satellite precipitation products in the Yellow River source region, China. J. Hydrol. 567, 696–711.
Yue, S., Ouarda, T., Bobee, B., 2001. A review of bivariate gamma distributions for hydrological application. J. Hydrol. 246 (1), 1–18.
Yusof, F., Hui-Mean, F., Suhaila, J., Yusof, Z., 2013. Characterisation of drought properties with bivariate copula analysis. Water Resour. Manag. 27 (12), 4183–4207.
Zhang, L., Singh, V., 2006. Bivariate flood frequency analysis using the copula method. J. Hydrol. Eng. 11 (2), 150–164.